

Novel method for determining ^{234}U - ^{238}U ages of Devils Hole 2 cave calcite (Nevada)

Xianglei Li¹, Kathleen A. Wendt^{1,2}, Yuri Dublyansky², Gina E. Moseley², Christoph Spötl², R. Lawrence Edwards¹

5 ¹Department of Earth Sciences, University of Minnesota, 116 Church Street SE, Minneapolis 55455, USA

²Institute of Geology, University of Innsbruck, Innrain 52, 6020 Innsbruck, Austria

Correspondence to: Xianglei Li (li000477@umn.edu)

Abstract. Uranium-uranium (^{234}U - ^{238}U) disequilibrium dating can determine the age of secondary carbonates over greater
10 time intervals than the well-established ^{230}Th - ^{234}U dating method. Yet it is rarely applied due to unknowns in the initial $\delta^{234}\text{U}$
($\delta^{234}\text{U}_i$) value, which result in significant age uncertainties. In order to understand the $\delta^{234}\text{U}_i$ in Devils Hole 2 cave, Nevada,
we have determined 110 $\delta^{234}\text{U}_i$ values from phreatic calcite using ^{230}Th - ^{234}U disequilibrium dating. The sampled calcite was
deposited in Devils Hole 2 between 4 and 590 thousand years, providing a long-term look at $\delta^{234}\text{U}_i$ variability over time. We
then performed multi-linear regression among the $\delta^{234}\text{U}_i$ values and correlative $\delta^{18}\text{O}$ and $\delta^{13}\text{C}$ values. The regression allows
15 us to predict the $\delta^{234}\text{U}_i$ value of Devils Hole calcite based upon its measured $\delta^{18}\text{O}$ and $\delta^{13}\text{C}$. Using this approach and the
measured present-day $\delta^{234}\text{U}$ values of Devils Hole 2 calcite, we calculate 110 independent ^{234}U - ^{238}U ages. In addition, we used
newly measured $\delta^{18}\text{O}$, $\delta^{13}\text{C}$, and present-day $\delta^{234}\text{U}$ values to calculate 10 ^{234}U - ^{238}U ages that range between 676 and 731
thousand years, thus allowing us to extend the Devils Hole chronology beyond the ^{230}Th - ^{234}U -dated chronology while
maintaining an age precision of $\sim 2\%$. Our results indicate that calcite deposition at Devils Hole 2 cave began no later than
20 736 ± 11 thousand years ago. The novel method presented here may be applied to future speleothem studies in similar
hydrogeological settings, given appropriate calibration studies.

1 Introduction

The mid-20th century discovery of ^{234}U - ^{238}U disequilibrium in natural waters (Cherdyntsev, 1955; Isabaev et al., 1960; Thurber,
1962) unlocked a new geochronometer for sediments in marine and freshwater settings. The greatest limitation of the ^{234}U -
25 ^{238}U dating method, however, lies in the uncertainty of the initial $\delta^{234}\text{U}$ ($\delta^{234}\text{U}_i$), as shown in Eq. 1:

$$\delta^{234}\text{U}_i = \delta^{234}\text{U}_p \times e^{(\lambda_{234} T)} \quad (1)$$

where $\delta^{234}\text{U}_p$ refers to the present $\delta^{234}\text{U}$ value, $\delta^{234}\text{U}_i$ refers to the $\delta^{234}\text{U}$ value at the time of deposition, λ_{234} is the decay constant of ^{234}U , and T refers to the time elapsed since deposition. In marine settings, $\delta^{234}\text{U}_i$ can be approximated using the known excess ^{234}U activity in seawater. Ku (1965) was the first to test the ^{234}U - ^{238}U geochronometer in marine sediments.

30 Although this method has been applied successfully in marine-sourced secondary carbonates (Veeh, 1966; Bender et al., 1979; Ludwig et al., 1991), it has largely been limited by the potential mobility of uranium following deposition, as observed in mollusks (Kaufman et al., 1971) and corals (Bender et al., 1979; Gallup et al., 1994).

In freshwater settings, constraining the $\delta^{234}\text{U}_i$ of secondary carbonates is further complicated by the fact that, in contrast to seawater, terrestrial surface and ground waters exhibit a wide spatial and temporal variability in $\delta^{234}\text{U}$. These uncertainties in

35 determining past $\delta^{234}\text{U}_i$ result in ^{234}U - ^{238}U age uncertainties that are orders of magnitude greater than those common for ^{230}Th - ^{234}U disequilibrium dating. ^{230}Th - ^{234}U dating has thus remained the preferred method for determining the age of secondary carbonates that have been deposited between modern day and ~600 thousand years (ka) before present (BP), when ^{230}Th and ^{234}U are very close to secular equilibrium. However, with a firm understanding of past source-water $\delta^{234}\text{U}_i$, the ^{234}U - ^{238}U disequilibrium method is a powerful geochronometer that can reach deeper in time than ^{230}Th - ^{234}U disequilibrium dating (e.g.

40 Gahleb et al., 2019).

Devils Hole (DH) and neighboring Devils Hole 2 (DH2) caves are ideal settings for the study of groundwater $\delta^{234}\text{U}_i$ variations over time. The walls of both steep fractures are coated with thick (up to ~90 cm) layers of calcite deposits that have precipitated subaqueously at a rate of approximately 1 mm per 1000 years (Ludwig et al., 1992; Moseley et al., 2016). Small variations in calcite $\delta^{234}\text{U}_i$ (1851-1616 ‰) over the last 500 ka BP have been precisely determined by Ludwig et al. (1992) and Wendt et al.

45 (2020). Due to the high initial ^{234}U excess in DH and DH2 calcite (mean $\delta^{234}\text{U}_i = 1750$ ‰), the ^{234}U - ^{238}U disequilibrium method can theoretically be applied to determine the age of DH and DH2 calcite as old as 2.5 million years.

Ludwig et al. (1992) were the first to calculate ^{234}U - ^{238}U ages from DH calcite. To do so, they derived the $\delta^{234}\text{U}_i$ value from 21 ^{230}Th - ^{234}U ages between 60-350 ka. From this dataset they calculated the median $\delta^{234}\text{U}_i$ value (1750 ‰) and associated uncertainty (± 100 ‰); the latter was derived from the range of $\delta^{234}\text{U}_i$ over the selected time period. Using this $\delta^{234}\text{U}_i$ value,

50 18 ^{234}U - ^{238}U ages were calculated. The ages ranged between 385-568 ka BP with mean uncertainties of 20 ka (3-5 % relative uncertainty) (Ludwig et al., 1992).

Building upon the pioneering work of Ludwig et al. (1992), we aim to decrease the uncertainties of DH and DH2 $\delta^{234}\text{U}_i$ in order to improve the precision of ^{234}U - ^{238}U ages. A negative correlation between DH $\delta^{234}\text{U}_i$ and $\delta^{18}\text{O}$, and a positive correlation between $\delta^{234}\text{U}_i$ and $\delta^{13}\text{C}$, is observed over the last 500 ka BP (Ludwig et al., 1992). Similar correlative patterns were obtained

55 over the last 200 ka BP using separate drill cores from DH2 (Moseley et al., 2016) and were shown to be independent of U

concentrations (Fig. S4; Wendt et al., 2020). In this study, we show that by accounting for changes in $\delta^{234}\text{U}_i$ with respects to $\delta^{18}\text{O}$ and $\delta^{13}\text{C}$, we can reduce the uncertainty in $\delta^{234}\text{U}_i$ by 35 %, thereby reducing the uncertainty in ^{234}U - ^{238}U ages to about \pm 13 ka within a several hundred-thousand-year range. We then use this method to calculate the age of calcite that was deposited in DH2 prior to (older than) the limit of ^{230}Th - ^{234}U disequilibrium dating (~600 ka BP). Doing so allows us to extend the radiometric chronology and determine the time at which calcite first deposited in DH2.

1.2 Regional Setting

DH and DH2 caves are located 100 m apart in a detached area of Death Valley National Park in southwest Nevada (36°25' N, 116°17' W; 719 m above sea level). Bedrock of the study area is composed of carbonates from the Bonanza King Formation of middle and late Cambrian age (Barnes and Palmer, 1961). The caves follow a pair of deep, planar, steeply dipping fault-controlled open fissures roughly 5 m wide, 15 m long, and at least 130 m deep (Riggs et al., 1994). Evidence for the tectonic origin of these caves includes the spreading and the orientation of their planar opening, which is perpendicular to the northwest-southeast principal stress direction that has prevailed in this part of the Great Basin for the last 5 million years (Carr, 1974). Parts of these extensional fractures were later modified by condensation corrosion (Dublyansky & Spötl, 2015).

DH and DH2 both intersect the water table of the Ash Meadows Groundwater Flow System (AMGFS), which is a large (~12,000 km²) aquifer hosted in Paleozoic limestones (Winograd and Thordarson, 1975). The AMGFS is primarily recharged by infiltration of snowmelt and rainfall in the upper elevations of the Spring Mountains (~500 mm a⁻¹; Winograd and Thordarson, 1975; Thomas et al., 1996; Winograd et al., 1998; Davisson et al., 1999). Quaternary extensional tectonics in this area has produced an underground network of open fractures which contribute to the high transmissivity of the aquifer. Previous studies suggest groundwater transit times of < 2000 years from the Spring Mountains to DH/DH2 caves (Winograd et al., 2006). Due to the long flow path (> 60 km) and prolonged residence time, the groundwater flowing southwest through both caves is very slightly supersaturated with respect to calcite (SI = 0.2; Plummer et al., 2000). The caves are < 1.5 km upgradient from a line of springs that represent the primary discharge area of the AMGFS.

Calcite has been continuously depositing as dense mammillary crusts on the submerged walls of DH and DH2 over much of the last 1 million years at a very slow rate of roughly 1 mm ka⁻¹ (Ludwig et al., 1992; Winograd et al., 2006; Moseley et al., 2016). The thickness (\leq 90 cm) of mammillary calcite crusts implies a long history of calcite-supersaturated groundwater. Regional groundwater transmissivity is maintained despite calcite precipitation due to active extensional tectonics (Riggs et al., 1994).

2 Methods

A 670 mm-long core was drilled from the hanging wall of DH2 cave at + 1.8 m relative to the modern water table (r.m.w.t.). The first 654 mm of the core consists of calcite; the last 16 mm of the core consists of bedrock. The core consists of two types

of calcite: mammillary calcite and folia. For a full description of the petrographic and morphological differences between both forms of calcite see Wendt et al. (2018). Briefly, mammillary calcite precipitates subaqueously, while folia forms at the water table in a shelf-like formation. The presence of folia in the core is an indicator of the paleo-water table near + 1.8 m r.m.w.t. at the time of deposition.

90 The selected core was cut longitudinally and polished. The core was surveyed for growth hiatuses and features indicative of changing deposition mechanisms and rates (such as folia). Folia was identified at 77.7-97.4 mm (as reported in Moseley et al., 2016), 171.4-199.2 mm, 209.4-229.0 mm, and 305.0-323.0 mm (distances are reported from top of the calcite sequence). In addition, a growth hiatus was discovered between 587.4 and 589.0 mm (supplementary Fig. 1).

The mammillary calcite portions of the core were ^{230}Th - ^{234}U dated at regular intervals ($n = 110$). As described in Moseley et al. (2016), folia calcite cannot be reliably dated. Results for the first 91 ^{230}Th - ^{234}U ages were published by Moseley et al. (2016) and Wendt et al. (2020). Nine additional ^{230}Th - ^{234}U ages were measured between 351.0 and 562.0 mm using identical methodology to the aforementioned publications. The purpose of additional ^{230}Th - ^{234}U ages is to extend the DH2 chronology toward secular equilibrium (about 600 ka BP). Between 608.2-652.0 mm, 10 new $\delta^{234}\text{U}$ measurements were collected for this study. To do so, calcite powders were hand drilled at approximately 1 cm intervals and spiked following the ^{230}Th - ^{234}U dating method cited above. The uranium aliquots were then extracted and measured following the methods described in Cheng et al. (2013). Chemical blanks were measured with each set of 10–15 samples and were found to be negligible (< 50 ag for ^{230}Th , < 100 ag for ^{234}U , and < 1 pg for ^{232}Th and ^{238}U).

Samples for stable isotope measurements were micromilled continuously at 0.1-0.2 mm intervals along the core axis between 0 and 158 mm and presented by Moseley et al. (2016). The values of two to three stable isotope measurements (0.1-0.2 mm in width) were averaged in order to pair with ^{230}Th - ^{234}U subsamples, which averaged 0.3 to 0.5 mm in width. Between 169.8-652.0 mm, 66 new stable isotope samples were micromilled at the location of each ^{230}Th - ^{234}U and $\delta^{234}\text{U}$ measurement published by Wendt et al. (2020). Similarly, 2-3 stable isotope measurements were averaged to encompass the width of uranium isotope subsamples. Calcite powders were analyzed using a Delta V plus isotope ratio mass spectrometer interfaced with a Gasbench II. Values are reported relative to VPDB with 1-sigma precisions of 0.06 and 0.08‰ for $\delta^{13}\text{C}$ and $\delta^{18}\text{O}$, respectively.

110 A statistical model was built to predict $\delta^{234}\text{U}_i$ values using $\delta^{18}\text{O}$ and $\delta^{13}\text{C}$ based on the correlation observed between measured $\delta^{234}\text{U}_i$ and stable isotope values from 4 to 590 ka BP. To calculate the correlation analysis for unevenly spaced time series, we chose the Fortran 90 program PearsonT3, which can provide the 95% calibrated confidence intervals (Olafsdottir and Mudelsee, 2014). Software OriginPro (version 2015) was used to conduct the regression analyses (Moberly et al., 2018; see detailed description in the supplementary method). Several types of models fitted with linear, quadratic, and cubic regression methods were built. The model that provided the best estimate of the measured $\delta^{234}\text{U}_i$ values was selected. Using this model, a

statistically derived (SD) $\delta^{234}\text{U}_i$ value can be generated based on known $\delta^{18}\text{O}$ and $\delta^{13}\text{C}$ values. The SD $\delta^{234}\text{U}_i$ and measured $\delta^{234}\text{U}_p$ can then be used to calculate ^{234}U - ^{238}U ages (Eq. 1). The ^{234}U decay constant of $2.82206 \pm 0.00302 \cdot 10^{-6} \text{ a}^{-1}$ (Cheng et al., 2013) was used. We validated our methodology and uncertainty estimates by comparing ^{230}Th - ^{234}U and ^{234}U - ^{238}U dates obtained for samples younger than 590 ka BP.

- 120 Using this dataset, we calculated 120 ^{234}U - ^{238}U ages for samples in total. With these ^{234}U - ^{238}U ages as input, we calculated an age model using the Bayesian statistical software OxCal version 4.2 (Bronk Ramsey and Lee, 2013). Age models were calculated under deposition sequence “P” with k-parameter set to 0.1 (Bronk Ramsey and Lee, 2013). The positions of growth hiatuses, including folia calcite, were incorporated into the age model as growth boundaries.

3 Results

- 125 The new ^{230}Th - ^{234}U disequilibrium ages (denoted in subsequent text as ^{230}Th ages for simplicity) are in stratigraphic order within uncertainties. ^{238}U and ^{232}Th concentrations fall within the range of previous data published by Moseley et al. (2016) and Wendt et al. (2020). The time-depth consistency and reproducibility of ages argue against open-system processes. The existence of a ca. 67-ka-long growth hiatus between 587.4-589.0 mm is supported by ^{234}U - ^{238}U ages (see supplementary materials).
- 130 In this study we split the $\delta^{234}\text{U}_i$ dataset into three sections (4-309 ka, 309-355 ka and 355-590 ka BP). The sections were divided according to the level of uncertainty in $\delta^{234}\text{U}_i$ derived from ^{230}Th ages (see Table 1 and Supplementary Table 4). The average $\delta^{234}\text{U}_i$ was the same within uncertainties regardless of how we grouped the data, implying no detectable trend in $\delta^{234}\text{U}_i$ with time.

Table 1: Statistics of $\delta^{234}\text{U}_i$ with different temporal groupings.

Time range in ka BP (# of samples)	Average $\delta^{234}\text{U}_i$ (‰)	Standard deviation of population (‰, 2σ)	Average precision (‰, range)
4-309 (66)	1761	99	5 (2-14)
309-355 (15)	1758	71	22 (13-33)
355-590 (29)	1787	120	50 (15-162)

- 135 DH2 oxygen isotope values reveal a negative correlation with $\delta^{234}\text{U}_i$ over the last 590 ka BP (0-578 mm along the core axis; $r = -0.52$ with the 95% confidence interval of $[-0.81; -0.06]$), whereas carbon isotopes reveal a positive correlation ($r = 0.71$ with the 95% confidence interval of $[0.57; 0.81]$; Fig. 1 and Table 2). The interpretation of $\delta^{18}\text{O}$ and $\delta^{13}\text{C}$ in DH and DH2 calcite has been extensively debated in Winograd et al. (1988, 1992, 2006), Coplen et al. (1994), and Moseley et al. (2016). DH/DH2 $\delta^{18}\text{O}$ is a reflection of meteoric precipitation at the principal recharge zones of the AMGFS. Modern meteoric $\delta^{18}\text{O}$ varies

140 seasonally by >10‰ in southern Nevada (Ingraham et al., 1991). Winter precipitation (−12 to −14‰ VSMOW) is sourced from the Pacific and provides the dominate fraction (~90%) of aquifer recharge, while summer precipitation (0 to −3‰ VSMOW) is sourced from monsoonal systems from the Gulfs of Mexico and California (see Winograd et al., 1998 for details). We interpret past variations in DH/DH2 $\delta^{18}\text{O}$ to be the result of (i) changes in temperature and variations in the path-length of moisture transport through Rayleigh fractionation processes, (ii) changes in $\delta^{18}\text{O}$ values at moisture source regions, and (iii)

145 changes in the relative contributions of summer versus winter precipitation (see Moseley et al., 2016 for details). Past DH/DH2 $\delta^{13}\text{C}$ variations have been argued to reflect the extent and density of vegetation in the recharge zones of AMGFS, such that $\delta^{13}\text{C}$ minima correspond to periods of maximum vegetation (Coplen et al. 1994).

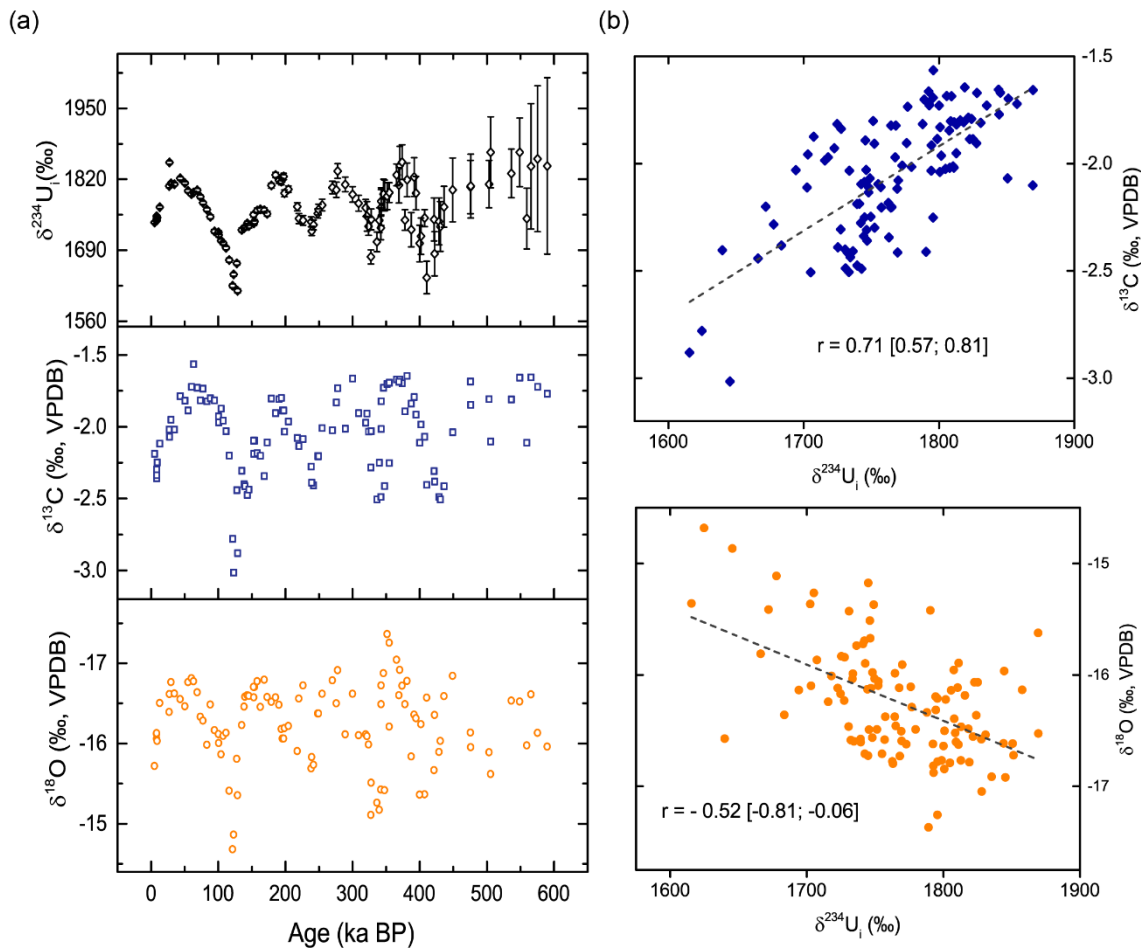


Figure 1: (a) Plots of DH2 ^{230}Th -derived $\delta^{234}\text{U}_i$, $\delta^{13}\text{C}$, and $\delta^{18}\text{O}$ over the last 590 ka BP; (b) scatter plots between DH2 ^{230}Th -derived $\delta^{234}\text{U}_i$ and $\delta^{13}\text{C}$, and ^{230}Th -derived $\delta^{234}\text{U}_i$ and $\delta^{18}\text{O}$ respectively. Correlation coefficients (r) with 95% calibrated confidence intervals and fitting curve (dashed lines) are shown.

The linear relationships presented here are consistent with results from Moseley et al. (2016) and Ludwig et al. (1992) in DH2 and DH cave, respectively. The anti-correlation between $\delta^{18}\text{O}$ and $\delta^{234}\text{U}_i$ is consistent with the interpretation presented in Wendt et al. (2020) such that periods of increased regional moisture availability (due to cooler, wetter conditions favoring depleted $\delta^{18}\text{O}$ values) are associated with increased DH $\delta^{234}\text{U}_i$ values. A full list of correlation calculations among $\delta^{234}\text{U}_i$, $\delta^{18}\text{O}$ and $\delta^{13}\text{C}$ is presented in Table 2. The linear relationship between $\delta^{13}\text{C}$ and $\delta^{234}\text{U}_i$ is closer than that between $\delta^{18}\text{O}$ and $\delta^{234}\text{U}_i$ for the same period. This is likely due to the fact that $\delta^{13}\text{C}$ and $\delta^{234}\text{U}_i$ are forced by local processes, including changes in vegetation density at the principal recharge zone and groundwater interaction with bedrock in the aquifer. Since changes in the local environmental and hydrological regime are closely interconnected, we expect similar trends in the timing and pattern of $\delta^{13}\text{C}$ and $\delta^{234}\text{U}_i$ signals. In contrast, DH/DH2 $\delta^{18}\text{O}$ reflects the $\delta^{18}\text{O}$ of meteoric precipitation, which is sensitive to atmospheric temperatures and changes in moisture source (Winograd et al., 1998; Moseley et al., 2016). Evidence suggests no secular temperature changes in the local aquifer over the last several glacial-interglacial cycles (Kluge et al., 2014; J. Fiebig, pers. comm.), thus DH/DH2 $\delta^{18}\text{O}$ is expected to be minimally influenced by aquifer-related processes. Overall, we expect a greater scatter in the $\delta^{18}\text{O}$ vs. $\delta^{234}\text{U}_i$ regression due to the compounding forcings that influence $\delta^{18}\text{O}$ on a much larger spatial scale.

Table 2: Correlation coefficient (r) with the 95% calibrated confidence intervals (in brackets) for pairs of $\delta^{18}\text{O}$, $\delta^{13}\text{C}$, and $\delta^{234}\text{U}_i$.

Time range in ka BP (# of samples)	Correlation coefficient (r)		
	$\delta^{234}\text{U}_i$ - $\delta^{18}\text{O}$	$\delta^{234}\text{U}_i$ - $\delta^{13}\text{C}$	$\delta^{18}\text{O}$ - $\delta^{13}\text{C}$
4-590 (110)	-0.52 [-0.81; -0.06]	0.71 [0.20; 0.92]	-0.54 [-0.85; -0.00]
4-355 (81)	-0.64 [-0.90; -0.02]	0.69 [0.33; 0.88]	-0.61 [-0.83; -0.21]
4-309 (66)	-0.68 [-0.95; -0.17]	0.72 [0.20; 0.92]	-0.56 [-0.80; -0.12]

Note: All the 95% confidence interval does not cross zero, indicating that all the r values are significant.

From Table 2, we can see that the modulus value $|r|$ for $\delta^{18}\text{O}$ and $\delta^{234}\text{U}_i$ is greatest in the 4 to 309 ka BP dataset, which represents the time span with the highest precision $\delta^{234}\text{U}_i$ values. In contrast, the $|r|$ values for $\delta^{13}\text{C}$ and $\delta^{234}\text{U}_i$ are similar regardless of $\delta^{234}\text{U}_i$ precision. We therefore explored various time ranges and types of regressions in order to determine the most precise predictor of $\delta^{234}\text{U}_i$ based upon $\delta^{18}\text{O}$ and/or $\delta^{13}\text{C}$.

3.1 Regression Analysis

We evaluated the linear and polynomial (quadratic and cubic) regression methods primarily by calculating the coefficient of determination (COD), i.e. R^2 . The R^2 value represents the percentage of variation of the SD $\delta^{234}\text{U}_i$ in terms of the total of observed $\delta^{234}\text{U}_i$. To further compare the robustness between different models, we adjusted the R^2 values from the different numbers of predictors, i.e. the degree of freedom (DF) of the predictors. The adjusted R^2 (Adj. R^2) values is shown in Table 3. All models were calculated without considering the analytical uncertainty of $\delta^{234}\text{U}_i$ values (see the supplementary regression model for more information).

Among the various models, multiple linear regression (MLR) for the time period of 4-309 ka BP in terms of both $\delta^{18}\text{O}$ and $\delta^{13}\text{C}$ yielded the highest Adj. R^2 value of 0.61, such that over this time span the model accounts for 61 % of the $\delta^{234}\text{U}_i$ variability (Table 3). The corresponding equation is as follows (cf. Table 4):

$$\text{SD } \delta^{234}\text{U}_i = 1.2 \times 10^3 - 44 \times \delta^{18}\text{O} + 86 \times \delta^{13}\text{C} \quad (2)$$

Table 3: Adjusted R^2 values for different models with various regression analysis methods.

Time period in ka BP	$\delta^{18}\text{O}$	$\delta^{13}\text{C}$	Both
Linear Regression (Adj. R^2)			
4-590	0.23	0.50	0.52
4-355	0.41	0.48	0.54
4-309	0.46	0.52	0.61
Quadratic Regression (Adj. R^2)			
4-590	0.28	0.50	0.52
4-355	0.43	0.49	0.55
4-309	0.46	0.52	0.60
Cubic Regression (Adj. R^2)			
4-590	0.38	0.50	0.51
4-355	0.42	0.48	0.54
4-309	0.47	0.52	0.61

Note: the robustness of the regression model can be evaluated by the coefficient of determination (COD), R^2 , which is defined as $R^2 = 1 - (\text{residual sum of squares, RSS})/(\text{total sum of squares, TSS})$. Adj. $R^2 = 1 - (\text{RSS}/(\text{DF of residual})) / (\text{TSS}/(\text{DF of total predictors}))$.

We then applied statistical methods to test the robustness of the chosen model, starting with the F test. The F value is the ratio of the mean square of the fitted model to the mean square of the residual. A ratio that deviates greatly from 1 indicates that the model differs significantly from the ‘y = constant’ model. The test returned $F = 52.5$, far larger than the critical value of the F test at a significance level of $\alpha = 0.01$ (DF of numerator = 2; DF of denominator = 65) ($F_{\text{crit}} = 4.95$), indicating that the model is tenable. Additional confidence in the robustness of the chosen model is derived from the autocorrelation results (see supplementary information).

Table 4: T test table of the multiple linear regression model for 4-309 ka BP.

Parameters	Value	Standard Error	t value	p value
Intercept	1.2E3	1.9E2	6.5	1.8E-08
Factor of $\delta^{18}\text{O}$	-44	10	-4.3	6.3E-05
Factor of $\delta^{13}\text{C}$	86	16	5.3	1.4E-06

Note: 1) the standard error of fitting parameters was calculated based on the standard deviation of the residual from the model and used only for t test; 2) a smaller p value represents a decreased likelihood that the parameter is equal to zero.

Second, we performed a “t-test” to check if every term in the MLR for 4-309 ka is significant. The t value is the ratio of the fitted value to its standard error. As shown in the Table 4, all the fitted values (coefficients and intercept) are significant at a significance level of $\alpha = 0.001$. Thus, we conclude the regression model to be robust.

3.2 Residual Analysis

We now estimate the uncertainty of the SD $\delta^{234}\text{U}_i$ values over the past 309 ka by analyzing the residuals, which is defined as the differences between the observed and predicted values. Figure 2 reveals that the residuals are approximately normal in distribution. Thus, we conclude that the regression model captures the dominant characteristic of variability in the observed values. The estimate of the residuals yields uncertainty of $\pm 60.5\%$ (95 % confidence interval) with an average of essentially zero ($4.4\text{E-}13$). We take the $\pm 60.5\%$ value to represent a constant uncertainty for all the SD $\delta^{234}\text{U}_i$ values, amounting to a $\sim 40\%$ reduction in $\delta^{234}\text{U}_i$ uncertainties (the original estimate of uncertainty from Ludwig et al. (1992) was 100 %). The analytical uncertainty of ^{230}Th -derived $\delta^{234}\text{U}_i$ is composite of (i) uncertainty of measured $\delta^{234}\text{U}_p$, which is incorporated into the ^{234}U - ^{238}U ages (see the following section), and (ii) the uncertainty of ^{230}Th ages, which is negligible relative to uncertainty of the model over the past 309 ka (see Table 1 and supplementary table 4). Thus we do not take this analytical uncertainty into account.

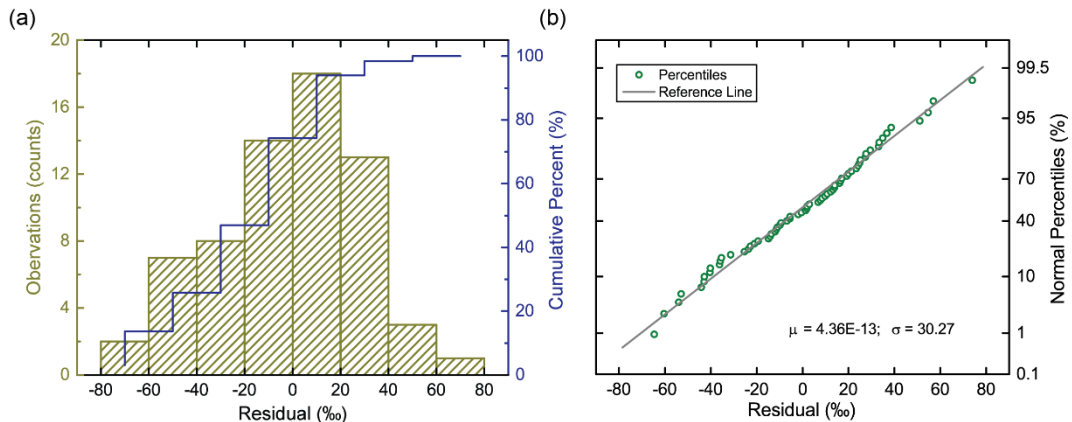


Figure 2: Histogram (left) and normal percentiles plot (right) of the residual. The reference line in the right plot refers to the line of standard normal distribution.

3.3 ^{234}U - ^{238}U Ages

Using Eq. 1 and 2, we then calculated the ^{234}U - ^{238}U disequilibrium ages (denoted in subsequent text ^{234}U ages for simplicity) for each data point for which $\delta^{234}\text{U}_p$, $\delta^{18}\text{O}$ and $\delta^{13}\text{C}$ are measured. The final uncertainty of ^{234}U ages comes from two sources: (i) the uncertainty of the model and (ii) the uncertainty in determination of $\delta^{234}\text{U}_p$. Combined, the final uncertainty of ^{234}U ages

215 before 590 ka BP is approximately ± 13 ka (2σ), which represents a 35 % improvement relative to previously reported ^{234}U
ages from DH (± 20 ka; Ludwig et al., 1992).

The ^{234}U and ^{230}Th ages between 4 to 590 ka BP are consistent within uncertainties (Fig. 3), with the exception of 4 ages (out
of 110) at 27 ka, 348 ka, 410 ka and 503 ka BP). Since uncertainties are reported at the 95 % confidence level, we would
expect this number of statistical outliers and conclude that our analysis is overall internally consistent. Alternately, there may
220 be some unknown underlying process not captured by our analysis which may be consistent with the variability of the residual
(see the supplementary figure 3).

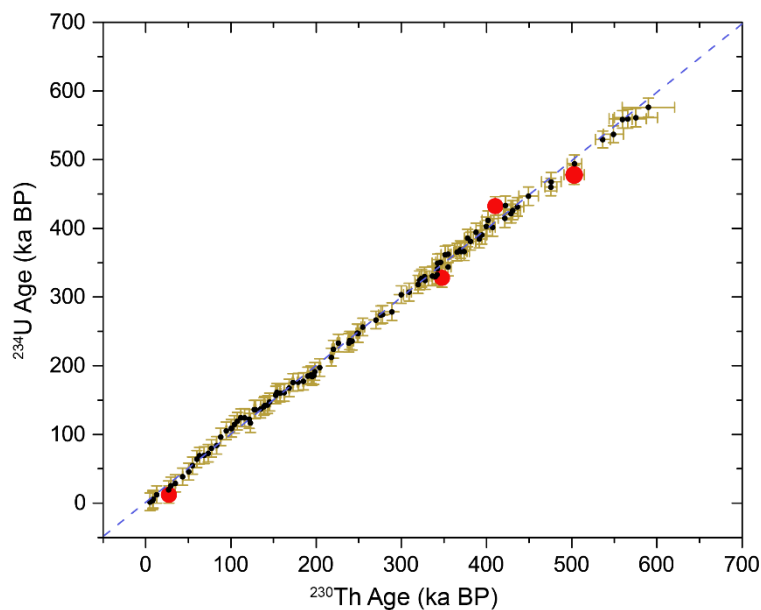


Figure 3: Plot of ^{234}U ages against ^{230}Th ages between 4 to 590 ka BP and the 2σ uncertainty shown by brown error bars. The dashed blue line is 1:1 line and the red dots refer to the points inconsistent between ^{230}Th and ^{234}U ages.

225 3.4 ^{234}U ages beyond ^{230}Th - ^{234}U secular equilibrium

The consistency between ^{234}U and ^{230}Th ages within the time range 4 to 590 ka BP suggests that it is reasonable to utilize this
model to calculate ages that are close to or beyond ^{230}Th - ^{234}U secular equilibrium in DH/DH2. Using measured $\delta^{234}\text{U}_p$, $\delta^{18}\text{O}$
and $\delta^{13}\text{C}$ values, we calculated 10 ^{234}U ages for DH2 cave deposits older than 600 ka BP over the depth of 608 to 652.0 mm
(Table 5). The ^{234}U ages are in stratigraphic order within uncertainty.

230

Table 5: SD $\delta^{234}\text{U}_i$ and calculated ^{234}U ages from calcite deposited prior to 600 ka BP and the corresponding depth, $\delta^{18}\text{O}$, $\delta^{13}\text{C}$ and $\delta^{234}\text{U}_p$ values.

Depth (mm)	$\delta^{18}\text{O}$ (‰, VPDB)	$\delta^{13}\text{C}$ (‰, VPDB)	$\delta^{234}\text{U}_p$ (‰)(2σ)	SD $\delta^{234}\text{U}_i$ (‰)(2σ)	^{234}U Age (ka BP)(2σ)
608.20	-16.22	-1.91	262.7 \pm 1.7	1773.3 \pm 60.5	676.4 \pm 14.4
611.80	-16.19	-1.81	262.1 \pm 1.9	1780.1 \pm 60.5	678.6 \pm 14.7
618.20	-15.96	-1.90	257.7 \pm 2.2	1762.2 \pm 60.5	681.1 \pm 15.2
623.40	-15.66	-2.00	247.6 \pm 1.6	1740.4 \pm 60.5	690.7 \pm 14.6
625.60	-15.53	-2.17	245.6 \pm 2.0	1719.9 \pm 60.5	689.5 \pm 15.4
630.00	-15.60	-1.99	241.0 \pm 1.5	1738.4 \pm 60.5	699.9 \pm 14.6
634.00	-16.29	-1.95	232.7 \pm 1.7	1773.1 \pm 60.5	719.3 \pm 14.7
638.00	-16.74	-1.87	229.4 \pm 1.5	1799.0 \pm 60.5	729.6 \pm 14.2
639.80	-16.13	-1.78	228.9 \pm 1.9	1780.0 \pm 60.5	726.5 \pm 14.9
652.00	-16.12	-1.92	229.4 \pm 1.8	1767.8 \pm 60.5	723.3 \pm 14.9

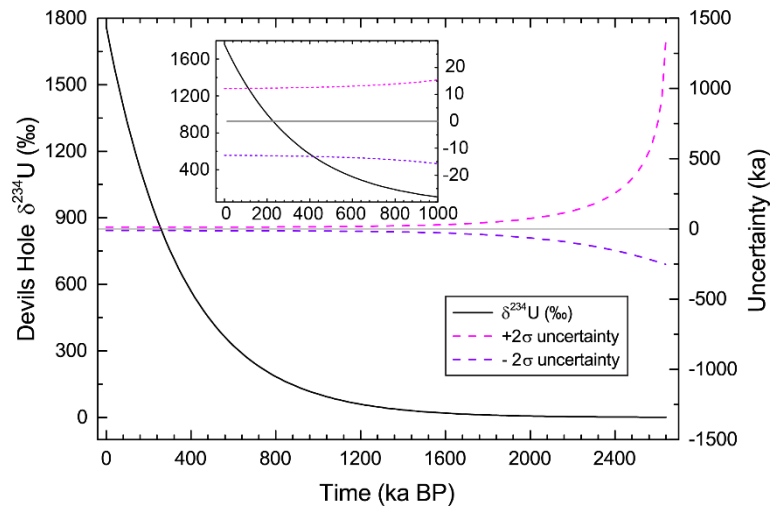
4 Discussion

4.1 Uncertainties of ^{234}U ages

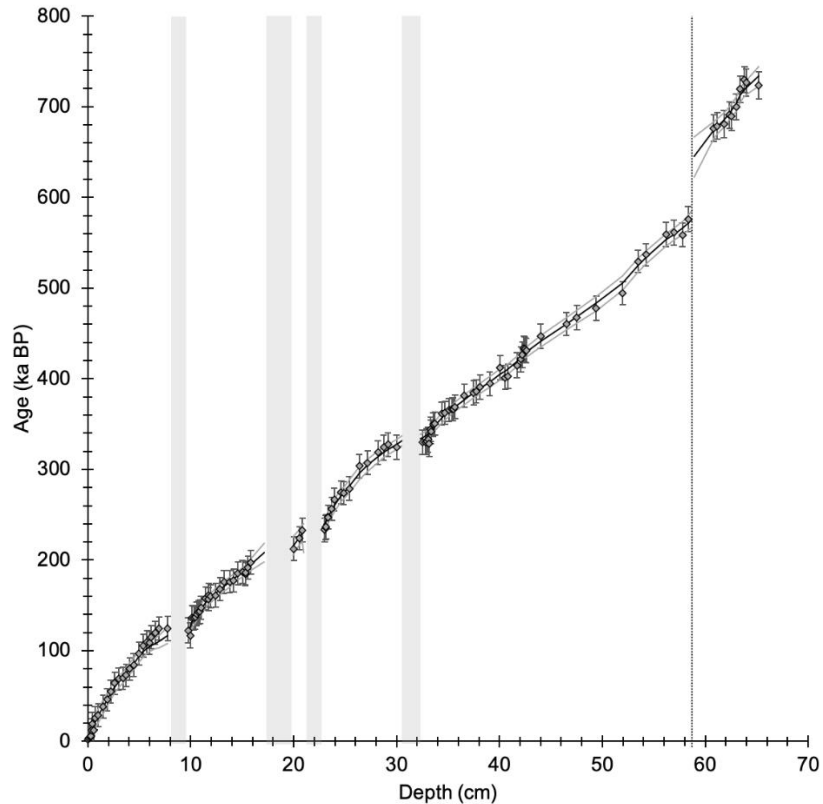
Due to the high initial $\delta^{234}\text{U}$ values (1760 ± 61 ‰), DH/DH2 calcite can theoretically be dated up to 2.5 million years (Ma) BP, assuming that measured $\delta^{234}\text{U}_p$ values have about 1 ‰ uncertainty. By including all the uncertainty above, we could obtain the following age uncertainty (2σ): ~13 ka uncertainty for a sample < 500 ka BP, 16 ka at 1.0 Ma BP, 26 ka at 1.5 Ma BP, 70 ka at 2.0 Ma BP and 290 ka at 2.5 Ma BP. The rapid increase in uncertainty after 2.5 Ma BP (Fig. 4) is due to the fact that ≥ 10 half-lives of the ^{234}U will have elapsed and the $\delta^{234}\text{U}_p$ values increasingly approach the uncertainty of their measurement.

4.2 Timing and rate of calcite deposition

Figure 5 shows an OxCal-derived age model with 95 % confidence intervals plotted over depth using all ^{234}U ages with their 2σ uncertainties. Location of folia and a growth hiatus are highlighted. Two lines of evidence suggest that the resulting time series is reasonable. Firstly, the average growth rate during the whole period is at 0.9 ± 0.3 mm ka^{-1} (1σ uncertainty; Fig. 6), which is consistent with growth rates reported by Moseley et al. (2016). Secondly, all ^{234}U ages are in stratigraphic order within uncertainties and fall within the 95 % confidence interval of our age model, implying no major outliers.



250 **Figure 4: Evolution of $\delta^{234}\text{U}$ and corresponding uncertainties of ^{234}U ages with time. The insert plot shows $\delta^{234}\text{U}$ evolution during the period of 0-1 Ma.**



255 **Figure 5: ^{234}U ages (diamonds) and associated 2σ uncertainties along the length of the core penetrating the calcite crust. OxCal age model (black line) and 95 % confidence limits (grey lines) were derived from ^{234}U ages. Location of folia (grey bars) and a growth hiatus (black dotted line) are indicated.**

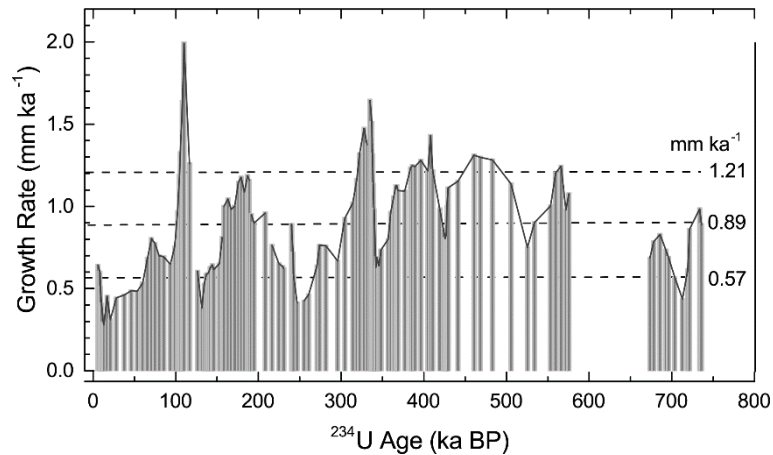
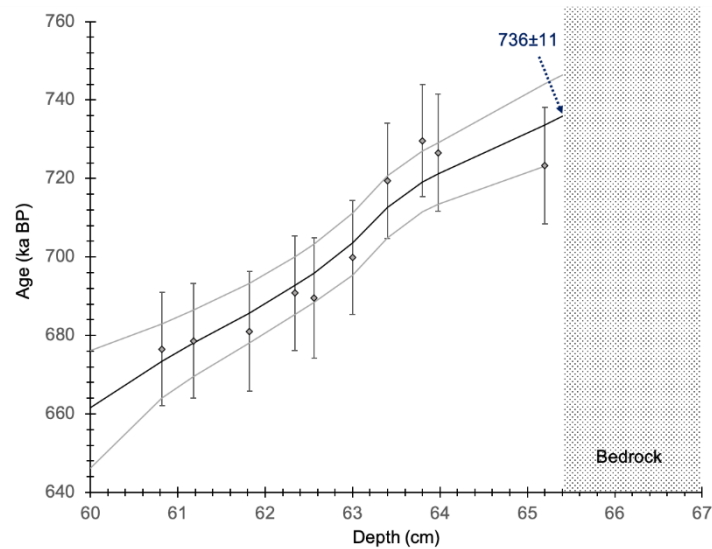


Figure 6: Growth rate of DH2 mammillary calcite based on the OxCal age model (cf. Fig. 6). The dashed lines indicate the average value and one standard deviation above and below the average.

Previous investigations revealed that DH2 cave opened to the surface at approximately 4 ka BP (Moseley et al., 2016), likely
 260 due to surface collapse processes (Riggs et al., 1994). The timing at which the main subsurface fissure opened, however,
 remains largely unknown. By ^{234}U dating the oldest calcite in our studied core (at the calcite-bedrock boundary), we can
 determine the earliest-possible timing at which the DH2 fissure existed (without which calcite cannot precipitate). ^{234}U ages
 in the last 170 mm of the core are in stratigraphic order within uncertainties (Fig. 7), yet due to the slight scatter of ages we
 utilize the OxCal age model to extrapolate the age at the calcite-bedrock boundary. In doing so, we determine the earliest
 265 calcite in this core (+ 1.8 m) to 736 ± 11 ka BP (Fig. 7).

The onset of calcite deposition in DH2 cave is in agreement with the recent geologic history of this region. The orientation of
 DH and DH2 is in accordance with the principal northwest-southeast stress direction in this part of the Great Basin that has
 prevailed over the last 5 Ma (Carr, 1974), suggesting that one or both fissures formed after 5 Ma BP. Abundant calcareous and
 siliceous spring and marsh deposits in Ash Meadows and the Amargosa Desert of Pliocene age (2.1 to 3.2 Ma BP; Hay et al.,
 270 1986) and groundwater-deposited calcite veins in alluvium and colluvium of Pleistocene age (500 to 900 ka BP; Winograd
 and Szabo, 1988) indicate that groundwater in the discharge zone of AMGFS has been continuously supersaturated with respect
 to calcite for at least the last 3 Ma. Our results, which suggest that the DH2 fissure opened no later than 736 ka BP, are therefore
 in agreement with the modern understanding of the AMGFS' geological history.



275 **Figure 7: OxCal-derived age model (black line), 95 % confidence limits (grey lines), ^{234}U ages (diamonds) with 2σ uncertainties for the lowest 17 cm of the core. The time series indicates that the initiation of calcite growth at the base of the core at 736 ± 11 ka BP.**

5 Conclusions

We have developed a novel method to determine the $\delta^{234}\text{U}_i$ values in DH/DH2 calcite. We established a MLR model between $\delta^{234}\text{U}_i$, $\delta^{18}\text{O}$, and $\delta^{13}\text{C}$ values of DH2 calcite deposited between 4 and 309 ka BP, and further tested the model over the time period of 309 and 590 ka BP. We applied this model to estimate the $\delta^{234}\text{U}_i$ of DH2 calcite using the respective $\delta^{18}\text{O}$ and $\delta^{13}\text{C}$ values. We refer to the statically derived initial values as SD $\delta^{234}\text{U}_i$. Uncertainty associated with SD $\delta^{234}\text{U}_i$ is ± 61 %, thereby improving precision by 40% relative to Ludwig et al. (1992). We then calculated 120 ^{234}U ages by determining the $\delta^{234}\text{U}_p$ and SD $\delta^{234}\text{U}_i$ at each age location. Average relative ^{234}U age uncertainties are 2%. The concordance between the ^{234}U and the ^{230}Th ages younger than 600 ka BP indicates that the DH2 calcite behaves as a closed system. 10 of the 120 ^{234}U ages are located in the oldest portion of the studied DH2 calcite core and range from 676 to 720 ka BP. Thus, the ^{234}U ages allow us to extend the DH2 chronology beyond the limits of ^{230}Th dating (>600 ka). Using our time series, we determined that calcite at the base of the studied core was deposited at 736 ± 11 ka BP. We argue that this age marks the earliest possible time at which the DH2 fissure existed.

Code/Data availability

290 All the data used in this paper are available in the supplementary tables.

Competing interests

The authors declare no competing financial interests that might have influenced the performance or presentation of the work described in this manuscript.

Author contribution

295 R.L.E. conceptualized the project and X.L. carried it out. K.A.W., X.L. and R.L.E. prepared the manuscript with contributions from all co-authors. X.L. did the formal analysis. C.S. and Y.D. provided the cave samples. K.A.W. and G.E.M. did the ²³⁰Th dating work and contributed to stable isotope measurements. All authors discussed the results and provided input to the manuscript and technical aspects of the analyses.

Acknowledgements

300 This work was supported by the National Science Foundation project number 1602940 (to R.L.E.) and the Austrian Science Fund (FWF) projects P263050 and P327510 (to C.S.). This research was conducted under research permit numbers DEVA-2010-SCI-0004 and DEVA-2015-SCI-0006 issued by the Death Valley National Park. We thank K. Wilson for assistance in the field and M. Wimmer for assistance in the laboratory. Finally, we would like to thank two anonymous reviewers for their insightful comments on this manuscript.

305 References

- Barnes, H. and Palmer, A.R.: Revision of stratigraphic nomenclature of Cambrian rocks, Nevada Test Site and vicinity, Nevada, U.S. Geological Survey Professional Paper, 424-C, 100-103, 1961.
- Bender, M.L., Fairbanks, R.G., Taylor, F.W., Matthews, R.K., Goddard, J.G., Broecker, W.S.: Uranium-series dating of the Pleistocene reef tracts of Barbados, West Indies, Geological Society of America Bulletin, 90, 577-594, [doi:10.1130/0016-7606\(1979\)90<577:UDOTPR>2.0.CO;2](https://doi.org/10.1130/0016-7606(1979)90<577:UDOTPR>2.0.CO;2), 1979.
- 310 Bronk Ramsey, C. and Lee, S.: Recent and planned developments of the program OxCal, Radiocarbon, 55, 720-730, [doi:10.2458/azu_js_rc.55.16215](https://doi.org/10.2458/azu_js_rc.55.16215), 2013.
- Carr, W.J.: Summary of Tectonic and Structural Evidence for Stress Orientation at the Nevada Test Site, U.S. Geological Survey Open-File Report, 74-176, [doi:10.3133/ofr74176](https://doi.org/10.3133/ofr74176), 1974.
- 315 Cheng, H., Edwards, R. L., Shen, C.-C., Polyak, V. J., Asmerom, Y., Woodhead, J., Hellstrom, J., Wang, Y., Kong, X., Spötl, C., Wang, X. and Alexander, E. C.: Improvements in ²³⁰Th dating, ²³⁰Th and ²³⁴U half-life values, and U-Th isotopic measurements by multi-collector inductively coupled plasma mass spectrometry, Earth Planetary Science Letters, 371–372, 82–91, [doi:10.1016/j.epsl.2013.04.006](https://doi.org/10.1016/j.epsl.2013.04.006), 2013.

- 320 Cherdyntsev, V.V.: Transactions of the third session of the commission for determining the absolute age of geological formations, *Izv Akad Nauk SSSR, Moscow*, 175–182, 1955.
- Coplen, T.B., Winograd, I.J., Landwehr, J.M. and Riggs, A.C.: 500,000-year stable carbon isotopic record from Devils Hole, Nevada, *Science*, 263, 361-365, [doi:10.1126/science.263.5145.361](https://doi.org/10.1126/science.263.5145.361), 1994.
- 325 Davisson, M.L., Smith, D.K., Kenneally, J., and Rose, T.P.: Isotope hydrology of southern Nevada groundwater: Stable isotopes and radiocarbon, *Water Resources Research*, 35, 279–294, [doi:10.1029/1998WR900040](https://doi.org/10.1029/1998WR900040), 1999.
- Dublyansky, Y., Spötl, C.: Condensation-corrosion speleogenesis above a carbonate-saturated aquifer: Devils Hole Ridge, Nevada, *Geomorphology*, 229, 17-29, doi.org/10.1016/j.geomorph.2014.03.019, 2015.
- Gallup, C., Edwards, R.L., and Johnson, R.: The timing of high sea levels over the past 200,000 years, *Science*, 263, 796-800, [doi:10.1126/science.263.5148.796](https://doi.org/10.1126/science.263.5148.796), 1994.
- 330 Ghaleb, B., Falguères, C., Carlut, J., Pozzi, J.P., Mahieux, G., Boudad, L., and Rousseau, L.: Timing of the Brunhes-Matuyama transition constrained by U-series disequilibrium, *Scientific Reports*, 9, 6039, doi.org/10.1038/s41598-019-42567-2, 2019.
- Hay R.L., Pexton R.E., Teague T.T. and Kyser T.K.: Spring-related carbonate rocks, Mg clays, and associated minerals in Pliocene deposits of the Amargosa Desert, Nevada and California, *Geological Society of America Bulletin*, 97, 1488-1503, [doi:10.1130/0016-7606\(1986\)97<1488:SCRMCA>2.0.CO;2](https://doi.org/10.1130/0016-7606(1986)97<1488:SCRMCA>2.0.CO;2), 1986.
- 335 Issbaev, E.A., Usatov, E.P. and Cherdyntsev, V.V.: Isotopic Composition of Uranium in Nature, *Radiokhimiya* (Engl. Transl.), 2, 1960.
- Kaufman, A., Broecker, W.S., Ku, T.-L. and Thurber, D.L.: The status of U-series methods of mollusk dating, *Geochimica et Cosmochimica Acta*, 35, 1155-1183, [doi:10.1016/0016-7037\(71\)90031-7](https://doi.org/10.1016/0016-7037(71)90031-7), 1971.
- 340 Kluge, T., Affek, H.P., Dublyansky Y. and Spötl, C.: Devils Hole paleotemperatures and implications for oxygen isotope equilibrium fractionation, *Earth and Planetary Science Letters*, 400, 251-260, [doi:10.1016/j.epsl.2014.05.047](https://doi.org/10.1016/j.epsl.2014.05.047), 2014.
- Ku, T.L.: An evaluation of the U^{234}/U^{238} method as a tool for dating pelagic sediments, *Journal of Geophysical Research*, 70, 3457-3474, [doi:10.1029/JZ070i014p03457](https://doi.org/10.1029/JZ070i014p03457), 1965.
- 345 Ludwig, K.R., Szabo B.J., Moore J.G. and Simmons K.R.: Crustal subsidence rate off Hawaii determined from $^{234}U/^{238}U$ ages of drowned coral reefs, *Geology*, 19, 171–174, [doi:10.1130/0091-7613\(1991\)019%3C0171:CSROHD%3E2.3.CO;2](https://doi.org/10.1130/0091-7613(1991)019%3C0171:CSROHD%3E2.3.CO;2), 1991.
- Ludwig, K.R., Simmons, K.R., Szabo, B.J., Winograd, I.J., Landwehr, J.M., Riggs, A.C. and Hoffman, R.J.: Mass spectrometric ^{230}Th - ^{234}U - ^{238}U dating of the Devils Hole calcite vein, *Science*, 258, 284–287, [doi:10.1126/science.258.5080.284](https://doi.org/10.1126/science.258.5080.284), 1992.
- 350 Moberly, J.G., Bernards, M.T. and Waynant, K.V.: Key features and updates for Origin 2018, *Journal of Cheminformatics*, 10, 5, [doi:10.1186/s13321-018-0259-x](https://doi.org/10.1186/s13321-018-0259-x), 2018.
- Moseley, G.M., Edwards, R.L., Wendt, K.A., Cheng, H., Dublyansky, Y., Lu, Y., Boch, R. and Spötl, C.: Reconciliation of the Devils Hole climate record with orbital forcing, *Science*, 351, 165–168, [doi:10.1126/science.aad4132](https://doi.org/10.1126/science.aad4132), 2016.

- 355 Olafsdottir, K. B., and Mudelsee, M.: More accurate, calibrated bootstrap confidence intervals for estimating the correlation between two time series, *Mathematical Geosciences*, 46, 411-427, [10.1007/s11004-014-9523-4](https://doi.org/10.1007/s11004-014-9523-4), 2014.
- Plummer, L.N., Busenberg, E. and Riggs, A.C.: In-situ growth of calcite at Devils Hole, Nevada: Comparison of field and laboratory rates to a 500,000 year record of near-equilibrium calcite growth, *Aquatic Geochemistry*, 6, 257–274. [doi:10.1023/A:1009627710476](https://doi.org/10.1023/A:1009627710476), 2000.
- 360 Riggs, A.C., Carr, W.J., Kolesar, P.T. and Hoffman, R.J.: Tectonic speleogenesis of Devils Hole, Nevada, and implications for hydrogeology and the development of long, continuous paleoenvironmental records, *Quaternary Research*, 42, 241–254, [doi:10.1006/qres.1994.1075](https://doi.org/10.1006/qres.1994.1075), 1994.
- Thomas, J.M., Welch, A.H. and Dettinger, M.D.: Geochemistry and isotope hydrology of representative aquifers in the Great Basin region of Nevada, Utah, and adjacent states, U.S. Geological Survey Professional Paper, 1409-C, [doi:10.3133/pp1409C](https://doi.org/10.3133/pp1409C), 1996.
- 365 Thurber, D.L.: Anomalous U^{234}/U^{238} in nature, *Journal of Geophysical Research*, 67, 4518-4520, [doi:10.1016/0079-6611\(65\)90016-9](https://doi.org/10.1016/0079-6611(65)90016-9), 1962.
- Veeh, H.H.: Th^{230} / U^{238} and U^{234}/U^{238} ages of Pleistocene high sea level stand, *Journal of Geophysical Research*, 71, 3379-86, [doi:10.1029/JZ071i014p03379](https://doi.org/10.1029/JZ071i014p03379), 1966.
- 370 Wendt, K.A., Dublyansky, Y.V., Moseley, G.E., Edwards, R.L., Cheng, H. and Spötl, C.: Moisture availability in the southwest United States over the last three glacial-interglacial cycles, *Science Advances*, 4, 10. [doi:10.1126/sciadv.aau1375](https://doi.org/10.1126/sciadv.aau1375), 2018.
- Wendt, K.A., Pythoud, M., Moseley, G.E., Dublyansky, Y.V., Edwards, R. L. and Spötl, C.: Paleohydrology of southwest Nevada (USA) based on groundwater $^{234}U/^{238}U$ over the past 475 k.y., *Geological Society of America Bulletin*, 132, 793-802. [doi:10.1130/B35168.1](https://doi.org/10.1130/B35168.1), 2020.
- 375 Winograd, I.J. and Thordarson, W.: Hydrogeologic and hydrochemical framework, south-central Great Basin, Nevada-California, with special reference to the Nevada Test Site, U.S. Geological Survey Professional Paper, 712-C, [doi:10.3133/pp712C](https://doi.org/10.3133/pp712C), 1975.
- 380 Winograd I.J. and Szabo B.J.: Water table decline in the south-central Great Basin during the Quaternary: Implications for toxic waste disposal, in: M.D. Carr, J.C. Yount (Eds.). *Geologic and Hydrologic Investigations of a Potential Nuclear Waste Disposal Site at Yucca Mountain, Southern Nevada*, U.S. Geological Survey Bulletin, 1790, 47-152, 1988.
- Winograd, I. J., Coplen, T.B., Landwehr, J.M., Riggs, A.C., Ludwig, K.R., Szabo, B.J., Kolesar, P.T. and Revesz, K.M.: Continuous 500,000-year climate record from vein calcite in Devils Hole, Nevada, *Science*, 258, 255–260, [doi:10.1126/science.258.5080.255](https://doi.org/10.1126/science.258.5080.255), 1992.
- 385 Winograd, I.J., Riggs, A.C. and Coplen, T.B.: The relative contributions of summer and cool-season precipitation to groundwater recharge, Spring Mountains, Nevada, USA, *Hydrogeology Journal*, 6, 77–93, [doi:10.1007/s100400050135](https://doi.org/10.1007/s100400050135), 1998.
- Winograd, I.J., Landwehr, J.M., Coplen, T.B., Sharp, W.D., Riggs, A.C., Ludwig, K.R. and Kolesar, P.T.: Devils Hole, Nevada, $\delta^{18}O$ record extended to the mid-Holocene, *Quaternary Research*, 66, 202–212, [doi:10.1016/j.yqres.2006.06.003](https://doi.org/10.1016/j.yqres.2006.06.003), 2006.